Coherent OCDMA Receivers with Robust Performance

Yi Yang[1], A. Brinton Cooper III[1], Jacob B. Khurgin[1], Jin U. Kang[1]

***Abstract*—Optical code division multiple access can achieve good spectral efficiency, a high degree of security, and soft degradation in many network applications. Robust performance in the presence of key impairments is achieved by careful selection of encoding sequences according to correlation properties and spread-time pulse shapes. A new, coherent receiver retrieves transmitted information coherently without phase locking or fast nonlinear detectors, while minimizing multiple access interference and cancelling beat noise. A key design improvement prevents link outage caused by random states of polarization without requiring polarization management.**

***Index Terms*—Optical fiber communication, OCDMA, multiple access interference, impairments, signature sequences**

I. INTRODUCTION

GROWING interest in optical code division multiple access (OCDMA) is driven by the need for increased flexibility, security, and throughput in applications that include network access and urban mesh backbone. Coherent receivers are required in order to minimize multiple access interference (MAI) and achieve cost-effective throughput. So-called "last mile" networks provide services to large numbers of end users, so the optical network unit (ONU) must be affordable and maintenance free. In the promising technique reported in [1], the pulse train from a mode-locked laser (MLL) is split into *M* identical signals, each spectrally phase encoded (SPE) with a distinct *signature sequence* drawn from a pair wise orthogonal set and modulated with information. A single fiber conveys the *M* signals through a passive network to the respective user ONUs. A second fiber carries the unencoded comb to each ONU, where it is encoded with the sequence of its target signal to form a local reference for correlation processing and information recovery without the need for a local optical source. This simple receiver uses a phase and polarization diversity (PPD) combiner [2] to effect coherent processing without using phase locking or fast, nonlinear optical devices. Beat noise is canceled and most MAI does not reach the photo detectors. This SPOT[2] architecture demonstrates high spectral efficiency and robustness to impairments [1].

However, a variety of factors can intervene to destroy the orthogonality between SPE signals, causing increased MAI and decreased throughput on the fiber link. For example, the relative delay between the arrival (on separate fibers) of data signal and reference comb undermines the orthogonality of the SPE signals, resulting in incomplete cancellation of MAI and reduced amplitude of the receiver output signal amplitude. In addition, robustness to fiber dispersion is impaired by SPE signals that concentrate energy at the pulse edges, causing significant intersymbol interference (ISI). Finally, lack of control of the state of polarization of both the data signal and the reference comb will lead to link outage in a significant portion of the OCDMA network.

Following a brief review of the SPOT system model in Section II, Section III presents a study of the relation between the properties of the SPE signals encoded by various signature sequences and the performance in the face of delay and dispersion. Section IV discusses the outages that are possible when signal and reference exhibit arbitrary SOP values from separate fibers and proposes a solution that avoids link outage without requiring the expensive or weakly-performing solutions mentioned above. Conclusions are drawn in Section V.

II. SPOT SYSTEM MODEL

As shown in Fig 1, a single MLL generates all the optical signals needed for one ``central office" or optical line terminal (OLT) to serve a population of *M* users. Consideration is restricted to the downlink. The ONU (Fig 2) encodes the reference comb with the sequence of the desired signal and demodulates the information using the PPD diversity combiner.

The received signal ensemble and encoded reference fields are given by (1a) and (1b), respectively, where *M* is the number of

$$E_S(t) = \sqrt{P_S}\cos\theta_S \sum_{m=1}^{M} A_m e^{j(\omega t+\phi_m)} c_m(t) \quad \text{(1a)}$$

$$E_\ell(t) = \sqrt{P_{LO}}\cos\theta_\ell e^{j(\omega t+\phi_\ell)} c_\ell(t) \quad \text{(1b)}$$

This work was supported by the US National Science Foundation under Grant ECCS-0925470 and was funded under the American Recovery and Reinvestment Act of 2009 (ARRA).

[1]Department of Electrical and Computer Engineering, The Johns Hopkins University, Baltimore, MD 21218, USA{yyang30,abcooper,jakek,jkangg@jhu.edu}

[2](**S**)PE (**P**PD) combining (**O**)CDMA (T)echnique

The modeling platform was the VPItransmissionMaker Optical Systems product offered by VPIsystems (http://www.VPIphotonics.com).

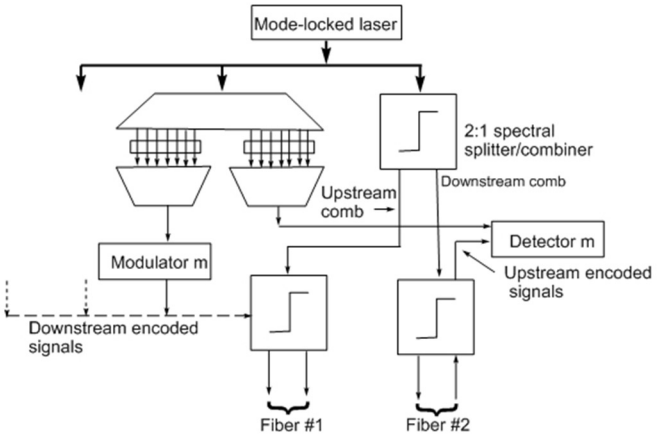

Fig 1. A single laser generates the downstream encoded signals for all the users served by a single ONU as well as the comb needed for the uplink.

users, S and l denote signal and "local," while P, ω, and ϕ, represent optical power, frequency, and phase. The m^{th} user's information bit is A_m, and θ is the polarization angle.

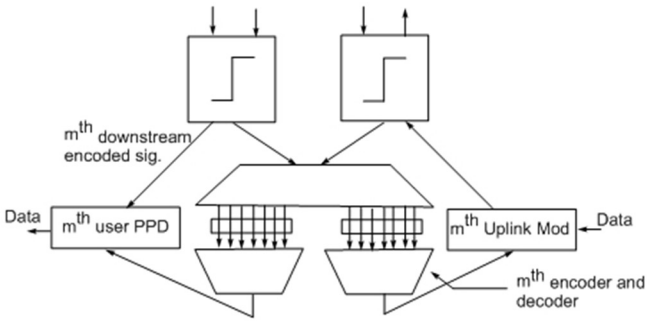

Fig. 2. Each ONU extracts the desired signal from the received ensemble using the PPD to effect correlation processing while canceling beat noise and MAI.

The signature sequences (2) are denoted $c_m(t)$ and, ideally, are pairwise orthogonal. This is explored further below.

$$c_m(t) = \sum_{n=-N/2}^{N/2} C_m^{(n)} e^{j\omega_n t}, m = 1,...,M, \omega_n = \omega_0 + \frac{2\pi n}{T} \quad (2)$$

Neglecting noise and slightly generalizing the development in [1] shows that the output of the PPD (Fig 7) in the absence of noise is

$$Y_1 = K[\cos^2\theta_S \cos^2\theta_l + \sin^2\theta_S \sin^2\theta_l] \quad (3)$$

III. ENCODING SEQUENCES

A. Introduction

This section shows how the properties of the time-spread SPE pulses impact the system bit error rate (BER) and how those properties are related to the selection of specific sequence families in the face of various impairments. SPE is affected by PSK modulation of the N central spectral lines of the optical pulse with a binary sequence of length N. *Hadamard* or H-sequences are of interest because any pair are orthogonal when fully synchronized (aligned) [14]. The N cyclic shifts of a *maximal length sequence* [15] constitute the family of *m-sequences* of length $N = 2^k - 1$ (integer k) which are nearly pairwise orthogonal and produce SPE waveforms that have more uniform energy distributions over a bit period than the others. The *Gold* or G-sequences [16] are also of length $N = 2^k - 1$ and were originally designed for a similar multiplexing application. Waveforms for representatives of each sequence family are shown in Fig. 3 for a data rate of 40 GHz and MLL pulse duration of 500 fs. All sequences have length N = 15 or 16.

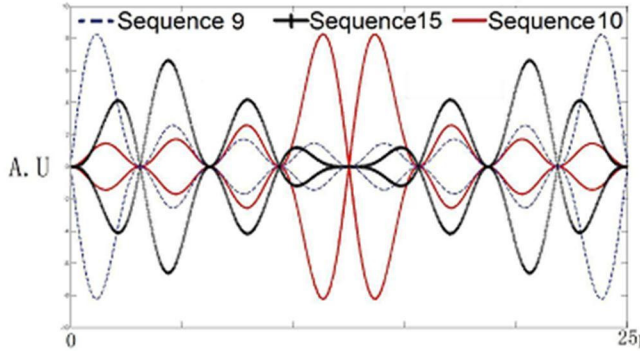

Fig 3a. Three H-sequences, N-16. Although pairwise orthogonal, they have very different distributions of pulse energy across the bit interval.

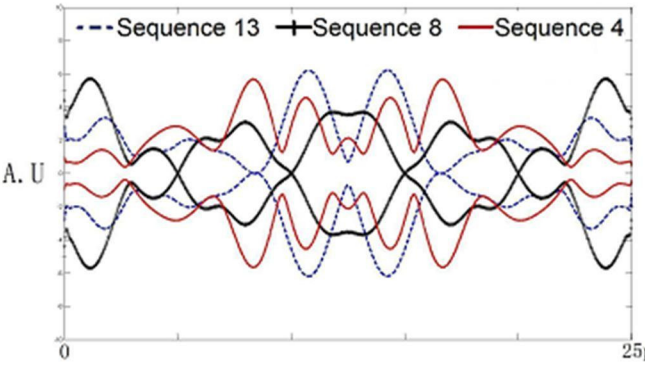

Fig 3b. Three G-sequences, N=16. The pulse excursions seem less extreme than those of the Hadamard sequences.

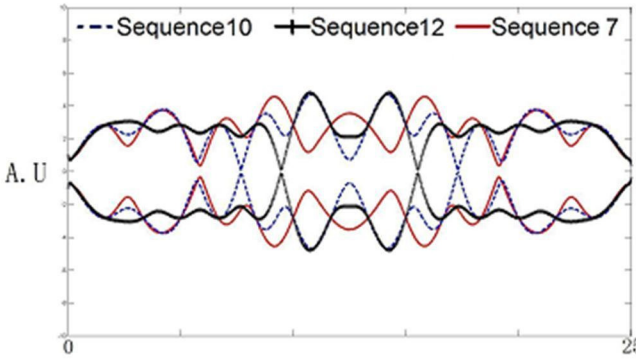

Fig 3c. Three m-sequences, N=15. These are the smoothest of the three families studied.

B. Noise and Impairments

The power efficiency curve (Fig. 4a) shows that the 18 dB SNR for a BER of 10^{-9} falls between the shot noise limit of 15.6 dB and the thermal noise limit of 21.6 dB [17]. In the simulations, delay and dispersion impairments were applied at

the point where the impairment-free SNR is 22 dB and the G- and m-sequences achieve a BER of 10^{-9}, thus giving adequate room to study the limitations imposed by impairments.

SNR Performance (No Impairments)

The BER for H-sequences (N =16) drops exponentially with SNR but for G- and m-sequences (N =15), BER exhibits an error floor for large SNR. In the noise-limited region (low SNR), BERs for all sequences converge (Fig. 4a).

Relative Delay

The information and local oscillator signals arrive on separate fibers, so perfect synchronization is unlikely. A 4-user system (*N=4*) using H- or m-sequences achieves BER < 10^{-9} for delays of about one pulse width (Figs. 4b and 4c).

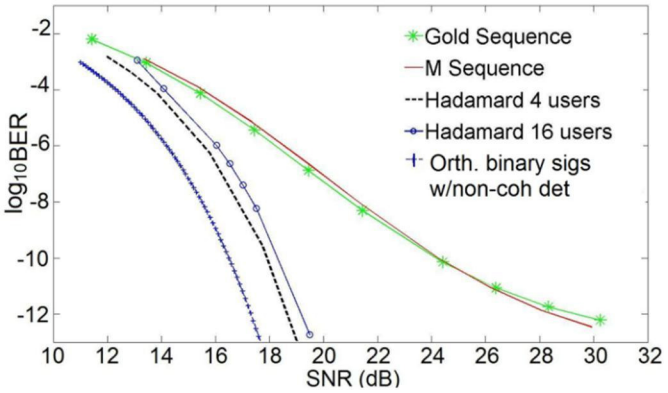

Fig 4a. BER vs. SNR for H-sequences, no impairments.

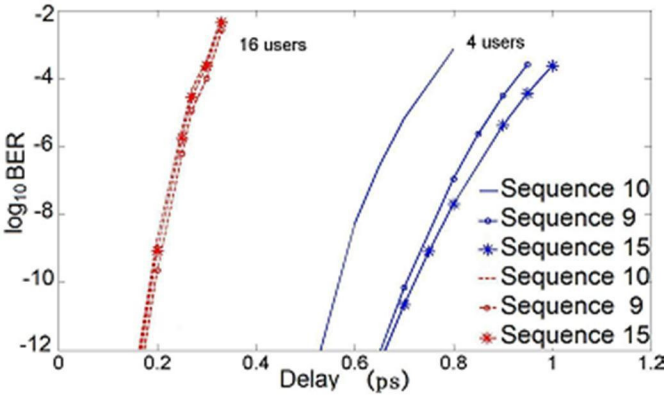

Fig 4b. . BER vs. relative delay for several H-sequences.

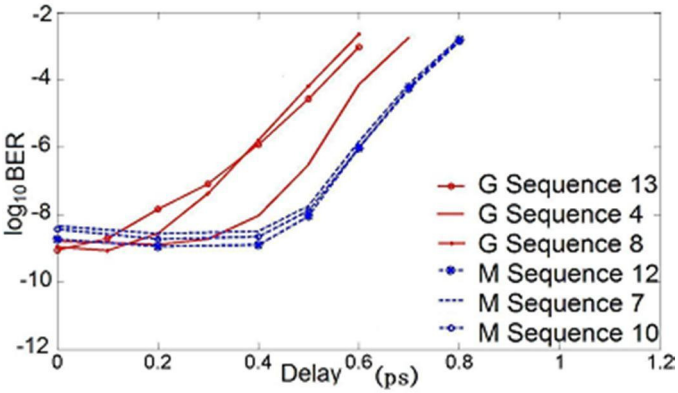

Fig. 4c BER vs relative delay for several m- and G-sequences.

BER vs. Total Dispersion

BER vs. total dispersion (TD) varies significantly from one sequence to another within each sequence family and among families as well (Fig. 5). Use of m-sequences provides BER < 10^{-9} for TD up to 5 ps. For H- and G-sequences, the BER appears to depend on the specific sequence used. Results for H- sequences (Fig 5a) indicate that SPE signals with pulse energy concentrated at the center of the pulse interval have higher tolerance to fiber dispersion. This is likely due to the small amount of energy in the dispersed signal's "tail" being carried into the adjacent pulse interval. For example, the pulse spread for sequence 10 (Fig. 3a) has a higher total fiber dispersion tolerance (25ps at BER=10^{-9}) than for sequence 9 (5ps at BER=10^{-9}).

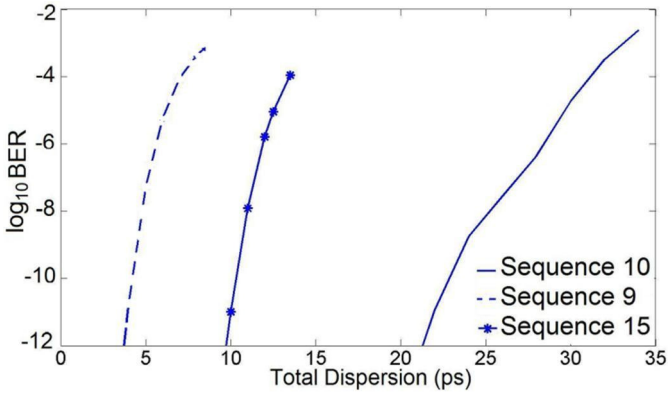

Fig. 5a. BER vs Total Dispersion for H-sequences.

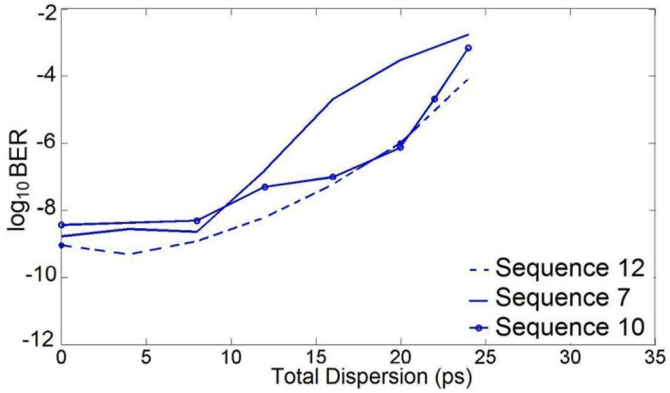

Fig. 5b. BER vs. Total Dispersion for m-sequences.

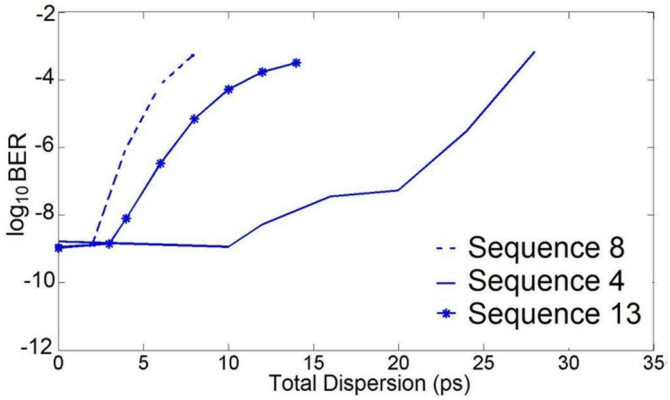

Fig. 5c. BER vs Total Dispersion for G-sequences

Although each H sequence has a different pulse spread, their total pulse energies are identical. To quantify the relation between dispersion tolerance and pulse shape, the pulse energy from the end to the center of each H sequence pulse is divided into 100 intervals, and the pulse value of each interval is sampled. An exponentially decaying weight is applied to these 100 values, and then they are summed and divided by the total pulse energy. This ratio not only indicates how much of the pulse energy is concentrated at the edge or center of each pulse spread, but also puts greater weight on energy located at pulse edge.

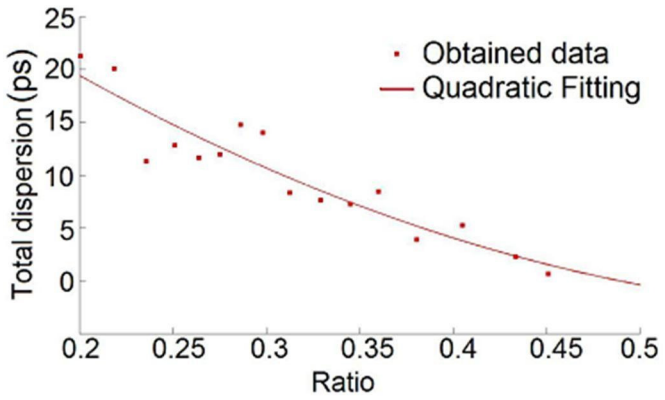

Fig. 5d. Maximum tolerated Total Dispersion for BER < 10^{-8} (H-sequences)

Fig 5d shows the maximum TD for which BER <10^{-8} plotted vs. this ratio. As shown, a higher ratio, meaning more pulse energy located at the pulse edge, has a lower fiber dispersion tolerance, and vice versa.

IV. THE PPD WITHOUT POLARIZATION MAINTENANCE

A. Discussion

Phase and polarization diversity combiners can tolerate polarization fluctuations in many cases [7], but unlike the referenced cases, the states of polarization of both the data signal and the reference comb are arbitrary (but assumed fixed). Significant efforts have been made [3] to maintain the SOP in fiber while accepting certain tradeoffs. For example, dissipative approaches result in non-negligible polarization dependent loss. Other approaches require nonlinear optics [4], optoelectronic elements for feedback systems [5], or nonlinear interactions between two counter propagating waves [3]. This work proposes a solution that avoids link outage without requiring the aforementioned expensive or weakly-performing solutions.

The original PPD structure is enclosed in dotted lines in Fig 6, where Y1 is the output. Let $K = 0.5R^2 P_S P_{LO} T^2$, where R is the photodiode responsibility, P_S is the user signal power at the PPD, P_{LO} is the reference signal power, θ_S and θ_{Lo} are the polarization angles of the signal and local oscillator light, and T is the information bit period. A slight generalization of the development in [2] gives (3) as reported above.

Depending on the values of θ_S and θ_{Lo} (*e.g.,* when $\theta_S = 0^o$ and $\theta_{Lo} = 90^o$) it is possible that $Y_1 = 0$; in this case, all of the signal power is directed to P1--P4 by the Wollaston prism, while local oscillator light power is directed to P5--P8. Therefore, no signal will be received and null output occurs.

$$
\begin{aligned}
Y_1 &= K(\cos^2\theta_S \cos^2\theta_{LO} + \sin^2\theta_S \sin^2\theta_{LO}) \\
Y_2 &= K(\cos^2(\theta_S + \pi/4)\cos^2(\theta_{LO} + \pi/4) \\
&\quad + \sin^2(\theta_S + \pi/4)\sin^2(\theta_{LO} + \pi/4)) \\
Y &= Y_1 + Y_2
\end{aligned}
\tag{4}
$$

The structure of the improved PPD is shown in Fig 6. Received signal and local oscillator light, with arbitrary SOPs, are split into two branches. Each branch is again split by a Wollaston prism. The prisms in the top branch split the light into orthogonally polarized states. In the bottom branch, the two Wollaston prisms are rotated in a way that the light is split into polarizations at 45° and 135° with reference to the top branch. Then all branches of light pass through 90° optical hybrids and the photodiodes (PD). An integrate and dump circuit operating at the data bit rate is placed behind each PD. The bit rate is 40GHz in this particular case. Finally the signals from each hybrid are subtracted, squared, and summed. The PPD output is then sampled at the bit rate.

When Y_1 is null, Y_2 will output the correct value. The null output is avoided through the summation of Y_1 and Y_2. When $\theta_S = 0^o$ and $\theta_{Lo} = 90^o$, Y1 outputs null, and Y = Y2 = K, thus avoiding the problem expressed in (3).

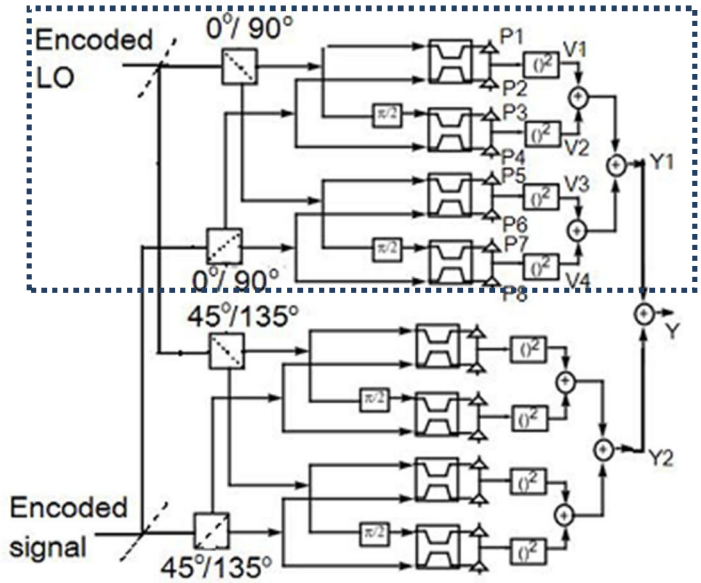

Fig. 6. Robust PPD combiner with signal rotations of 0 and π/4.

B. Simulation and Results

The simulation configuration described earlier applies here, with a length 16 Hadamard code [14] generating the SPE. The dark current value for the photodiode is set to 10nA, thermal noise is $5*10^{-14}$A/$\sqrt{Hz}$, and shot noise is proportional to the sum of the dark and signal currents [12]. The SNR is 22 dB. The value of Y is sampled at the very end of each 25 ps pulse period. The BER was estimated from the Q function [12], using the values of sample mean and variance conditioned on the transmitted binary symbol value.

Fig 7 shows the output of the PPD when signals are equally distributed among all detectors and giving optimal performance.

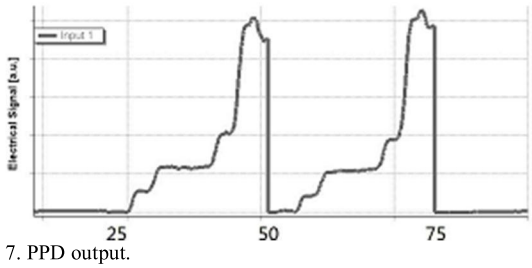

Fig 7. PPD output.

Figs 8a and 8b show the histograms of output values from the original and proposed PPDs. These were obtained by varying the polarization angles of signal and local oscillator light through all possible pairs of closely spaced, discrete values between 0 and 2π. As shown in Fig. 8a, the original PPD output ranges from 0 to 1, indicating that certain combinations of the SOP would result in null output. The proposed PPD output (Fig. 8b) ranges from 0.5 to 1.5, indicating that the null output problem is eliminated.

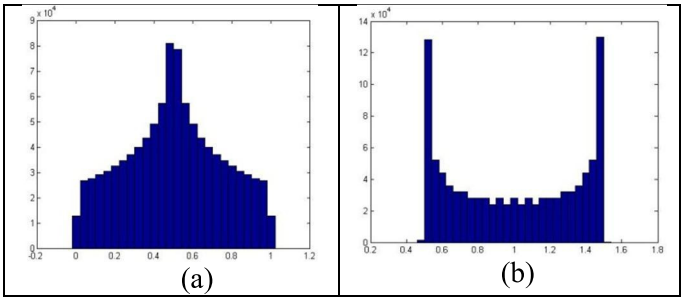

Fig.8(a). The output histogram of the original PPD. (b). The output histogram of the proposed PPD

The simulation shows that, when the output value falls below 0.25, the BER increases to 10^{-9}. Computing the fraction of points for which $Y < 0.25$ estimates that the probability that BER > 10^{-9} is 0.185. Fig 9 shows the fraction of combinations of SOP values as a function of the BER, based on the original PPD design.

Another view of the effect of SOPs on BER is obtained by placing a polarization controller on each of the simulated reference and user signal fibers. First, the signal fiber's SOP is set to 0^o, and BER is measured as the reference fiber's SOP varies from -90^o to 90^o. A second trial of BER is measured when the signal fiber's SOP is set to 30^o.

In Fig 10, stars (red dots) indicate BER vs. reference polarization angle when the polarization angle of the signal fiber is maintained at 0^o. The circles (blue dots) indicate the relationship when the signal fiber polarization angle is 30^o. With varying degrees of SOP imposed on the reference signal, the PPD was still able to retrieve data, and no null output was produced for any combination of values of θ_S and θ_{Lo}. In the study of PPD performance against reference polarization angle, the PPD avoided signal fading caused by varying SOP. Y does vary as θ_S and θ_{Lo} change, and the BER would reach lowest level as Y reaches maximum. The worst case BER is seen to occur (Fig. 10) at $\theta_S = 0$; $\theta_{Lo} = 45^o$, as expected, and perhaps at other pairs of angles as well.

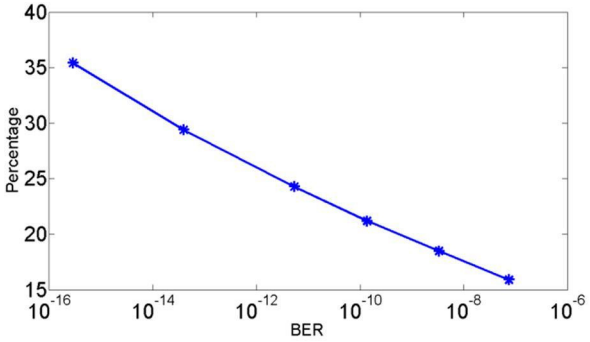

Fig. 9. Fraction of all links for which the BER exceeds certain values.

.

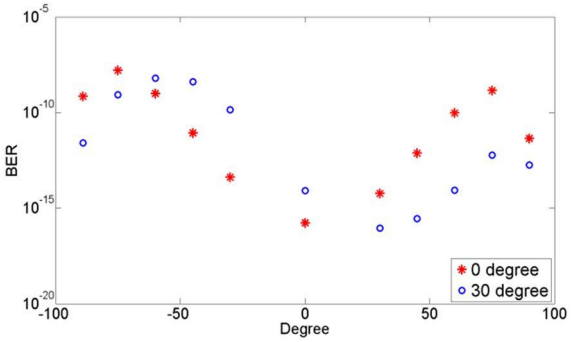

Fig. 10. BER vs. Reference Polarization Angle

However, in a real system this effect would not be so drastic since both θ_S and θ_{Lo} are arbitrary. This result coincides with the simulation of Y output based on equation (4). The BER value in Fig. 10 reaches maximum when the simulated Y output is lowest, and minimum when the simulated Y value is highest. The worst BER in Fig. 10 for the improved PPD is 10^{-9}. This is a substantial improvement compared to the original PPD where the worst BER is 0.5 when null output occurs.

V. DISCUSSION AND CONCLUSION

The sensitivity of SPOT performance to the selection of encoding sequences has been conclusively demonstrated. The sequences studied were chosen for their popularity, albeit in synchronous systems. In any practical implementation, it will not be possible to maintain the delay between data and reference signals to the 0.1 ps required by controlling the lengths of the distinct fibers carrying them. In a practical implementation, a manual delay adjustment using, *e.g.,* piezoelectric phase shifters, may sufficiently reduce the delay to obtain usefully small values of BER. But in any case, additional work on asynchronous SPOT is required. Even when perfect synchronism is assumed, the error floor exhibited by two sequence families shows that even small sequence cross correlation values have immense impact in a multiple access system which, as the examples clearly show, is MAI limited. Increasing received signal power has little effect on BER in such cases.

Because the delay and dispersion for most m- and G-

sequences are flat at minimum BER, these sequences offer much more robust performance with these impairments than the H-sequences, the slopes of which are steep throughout. SPOT waveforms with high energy concentration at the pulse edges are less tolerant of fiber dispersion. The attempt to quantify the relation between dispersion tolerance and pulse shape seems to support the conjecture. Thus, with carefully chosen sequences, impairments in coherent SPE-OCDMA can be successfully mitigated in some cases.

The improved PPD receiver for SPOT has been shown to solve the outage problem. Although the proposed design is more complex than the original, the alternatives of active SOP management using elaborate liquid crystal birefringent cells or Faraday magnetooptical effects combined with digital signal processing and control loops [5] introduce sensitive components preclude a robust design.

REFERENCES

[1] A. B. Cooper III, J. B. Khurgin, and J. K ang, “Phase and polarization diversity for OCDMA,” in Conference on Lasers and Electro Optics (CLEO) ’06, Optical Soc. of Amer., 2006.

[2] A. B. Cooper III, J. B. Khurgin, S. Xu, and J. U. Kang, “Phase and polarization diversity for minimum MAI in OCDMA networks,” IEEE J. Select. Topics in Quantum El., vol. 13, pp. 1386–1395, Sept. 2007.

[3] J. Fatome, S. Pitois, P.Morin, and G.Millot, “Observation of light-by-light polarization control and stabilization in optical fibre for telecommunication applications,” Optics Express, vol. 18, pp. 15311–15317, 2010.

[4] T.Sakamoto, H.-C. Lim, and K. Kikuchi, “All-optical polarization-insensitive time-division demultiplexer using a nonlinear optical loop mirror with a pair of short polarization-maintaining fibers,” IEEE Photon. Tech. Ltrs., vol. 14, pp. 1737–1739, Dec. 2002.

[5] M. Martinelli, P. Martelli, and S. Pietralunga, “Polarization stabilization in optical communications systems,” IEEE J. Lightwave Technol., vol. 24, pp. 4172–4183, Nov. 20

[6] K. Kikuchi, “Optical homodyne receiver comprising phase and polarization diversities with digital signal processing,” in Digest, IEEE/LEOS summer topical meetings, 2007, IEEE/LEOS, 2007.

[7] Kazovsky, L.G.; , "Phase- and polarization-diversity coherent optical techniques," *Lightwave Technology, Journal of* , vol.7, no.2, pp.279-292, Feb 1989

[8] Enning, B.; Vodhanel, R.S.; Dietrich, E.; Patzak, E.; Meissner, P.; Wenke, G.; , "Signal processing in an optical polarization diversity receiver for 560-Mbit/s ASK heterodyne detection," *Lightwave Technology, Journal of* , vol.7, no.3, pp.459-464, Mar 1989

[9] Okoshi, T.; Cheng, Y.H.; , "Four-port homodyne receiver for optical fibre communications comprising phase and polarisation diversities," *Electronics Letters* , vol.23, no.8, pp.377-378, April 9 1987

[10] Kreit, D.; Youngquist, R.C.; , "Polarisation-insensitive optical heterodyne receiver for coherent FSK communications," *Electronics Letters* , vol.23, no.4, pp.168-169, February 12 1987

[11] S. Etemad, T. Banwell, S. Galli, J. Jackel, R.Menendez, P. Toliver, and J. Young, “Optical-CDMA incorporating phase coding of coherent frequency bins: concept, simulation, experiment,” in OSA/OFC 2004, OSA, 2004.

[12] VPItransmissionmake&VPIcomponentMaker Photonic Modules Reference Manual.

[13] Etemad, S.; Banwell, T.; Galli, S.; Jackel, J.; Menendez, R.; Toliver, P.; Young, J.; Delfyett, P.; Price, C.; Turpin, T.; , "Optical-CDMA incorporating phase coding of coherent frequency bins: concept, simulation, experiment," *Optical Fiber Communication Conference, 2004. OFC 2004* , vol.2, no., pp. 1 pp. vol.2, 23-27 Feb. 2004

[14] A Hedayat, N. Sloane, and J. Stufken, Orthogonal arrays: theory and applications, New York: Springer, 1999.

[15] S. Golomb, *Shift Register Sequences,* Laguna Hills: Aegean Park Press, 1982.

[16] R. Gold,”Optimal binary sequences for spread spectrum multiplexing,” *IEEE Trans. Inform. Theory,* vol 13, pp 619-621, Oct 1967.

[17] G. Agrawal, Fiber-Optic Communications Systems. New York: Wiley Inter-Science, 2002.